ACS APPLIED MATERIALS & INTERFACES
RESEARCH ARTICLE
www.acsami.org

Controlled Growth of Well-Aligned GaS Nanohornlike Structures and Their Field Emission Properties

Godhuli Sinha,[†] Subhendu K. Panda,[†] Anuja Datta,[†] Padmakar G. Chavan,[‡] Deodatta R. Shinde,[‡] Mahendra A. More,[‡] D. S. Joag,[‡] and Amitava Patra[*,†]

[†]Department of Materials Science, Indian Association for the Cultivation of Science, Jadavpur-700 032, Kolkata, India

[‡]Center for Advanced Studies in Materials Science and Condensed Matter Physics, Department of Physics, University of Pune, Pune 411007, India

S *Supporting Information*

ABSTRACT: Here, we report the synthesis of vertically aligned gallium sulfide (GaS) nanohorn arrays using simple vapor−liquid−solid (VLS) method. The morphologies of GaS nano and microstructures are tuned by controlling the temperature and position of the substrate with respect to the source material. A plausible mechanism for the controlled growth has been proposed. It is important to note that the turn-on field value of GaS nanohorns array is found to be the low turn-on field 4.2 V/μm having current density of 0.1 μA/cm^2. The striking feature of the field emission behavior of the GaS nanohorn arrays is that the average emission current remains nearly constant over long time without any degradation.

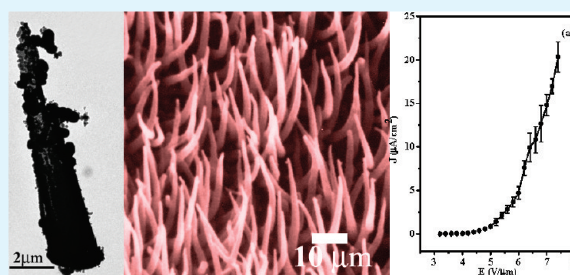

KEYWORDS: GaS nanohorn, 1D nanostructures, arrays, field emission, vapor−liquid−solid, photoluminescence

1. INTRODUCTION

Assemblies of chalocogenides semiconductor nanomaterials having layered crystal structures are very attractive because they have strong intralayer covalent bonding and interlayer weak van der Waals interaction, which lead to attractive for photovoltaic and optoelectronic applications.[1] The anisotropic bonding phenomenon also results in dangling bond only at the edge of the layers and enables commendable photostability.[2,3] Considerable progress has been made in the past few years for the fabrication of different layer-structured III−VI semiconductors in various nanoforms via chemical and physical processing techniques in controlled manner.[4,5] Among the III−VI group of semiconductor materials, gallium sulfide is one of the most important materials, with two different stoichiometries, i.e., GaS and Ga_2S_3. Hexagonal GaS, with direct wide band gap of 3.05 eV and indirect band gap of 2.5 eV, is more useful for optoelectronic applications.[6] GaS crystallizes in layered structure with double layer of nonmetal atoms, consisting of S−Ga−Ga-S sheets, stacking along *c* axis, having intralayer Van der Walls bonding and interlayer covalent bonding and is structurally similar to graphite.[7−9] GaS, having layered structure possesses a tendency of rolling up the molecular layer and form tubular structures along the basal plane.[10] The layered crystal structure of GaS has been the key essence behind synthesizing varieties of nanostructures like nanowalls, nanotube as have been reported by many groups.[9,11,12] However, GaS nanostructures with low crystal quality compared to bulk crystals may have detrimental effect on the semiconducting performance in the real devices. Previously, we have also synthesized very thin GaS nanobelts using catalyst-assisted thermal evaporation method and successfully maneuvered the bending of the growth direction of these nanobelts by controlling the diameter of catalytic droplets.[13] Shen et al.[14] reported precursor and substrate position dependent growth of GaS nanostructures. However, the systematic studies on the morphology of GaS nanostructures are still rarely available until now.

The research activities on the field-emission properties of nanomaterials now become the center of attention because of growing demands of micro and nanotechnologies. The desire of low turn on voltage and better emission current stability in ultra high vacuum condition leads to the use of different semiconductor 1D nanostructures.[1,15−19] Variation in the nature of the nanostructures by altering size, shape and density may have pronounced effects in the feature of field emission properties.[20,21] According to the Fowler−Nordheim (F−N) theory, the field emission is related to two essential parameters, such as the work function of the emitting material and the field enhancement factor.[22] However, as the work function is an intrinsic property it may not be altered for the particular inorganic semiconductor. On the other hand, the field-enhancement factor, which is the ratio of local field to the applied field, can be modified by altering the aspect ratio and tip diameter of the

Received: March 18, 2011
Accepted: May 9, 2011
Published: May 09, 2011

 © 2011 American Chemical Society

Scheme 1. Schematic Diagram of the Experimental Setup Used for Growth of GaS Nano- and Microstructures

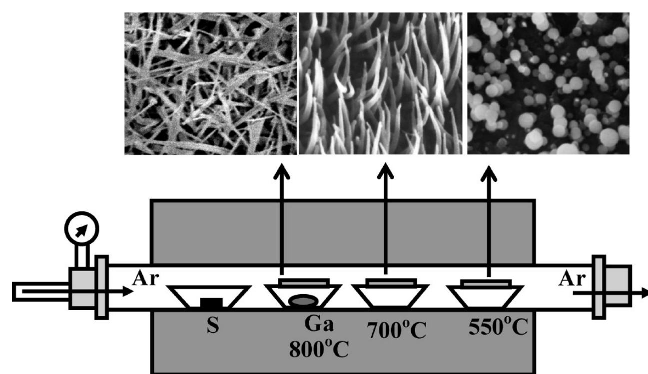

nanostructure. High aspect ratio and sharpness of the array component is reported to culminate enhanced field emission performances from array of ZnO nanoneedles.[20] Zhai et al.[1] reported the field emission behavior of arrays of different shaped CdS 1D nanostructures and showed that both of the alignments and aspect ratios greatly affected the field-emission properties. This results indicate that, it is possible to achieve better field emission characteristics from a given nanostructure material if it is long and sharp. Previously, we studied the field emission property of GaS nanobelts, and interestingly, these GaS nanobelts[13] captured attention by showing low turn on field (2.9 V/μm for 1 nA/cm^2) attributing to their high aspect ratio. Considering the importance of size and shape anisotropy dependent field emission properties and lack of systematic studies on the morphology of GaS, we explored the effect of position of the substrates with respect to the metal source and the substrate temperature in the formation of GaS 1D nanostructures.

Herein, we report the controlled synthesis of 1D GaS nanostructures using a catalytic VLS method. The morphologies of GaS nanowires, nanohorn arrays are controlled by tuning the temperature and position of the substrates from the metal precursor. Field emission investigations of the vertically aligned GaS nanohorns are found to be promising. These properties may be attributed to the good alignment and high aspect ratio of GaS nanohorns having sharp tips.

2. EXPERIMENTAL SECTION

The vapor liquid solid (VLS) method mediated synthesis process was performed in a horizontal tube furnace having different temperature zones. The synthesis was performed within a quartz tube of 4 cm diameter. High-purity Ar gas was used as a carrier gas with a flow rate of 100 sccm. In a typical process, the source materials gallium (Ga) metal and sulfur (S) powder were placed in separate quartz boats and positioned at the temperature of 800° and 450 °C respectively. Si (100) wafers, sputter-coated with a thin (~25 Å) layer of Au film, were used as the substrate and clipped to the quartz boats horizontally such that the Au-coated surface faced downward. One substrate is clipped to the boat containing Ga metal maintaining a vertical distance of nearly 5 mm from the Ga source and other two Si substrates were placed at 700 and 550 °C. The experimental set up is shown in scheme 1. After pumping the tube to base pressure of 8×10^{-2} mbar and purging the tube with Ar gas for 30 min, the tube was placed inside the preheated furnace. The deposition was continued for 20 min and then the tube was taken out from the furnace in order to arrest the further growth of the nanostructures. After cooling to room temperature under flowing Ar

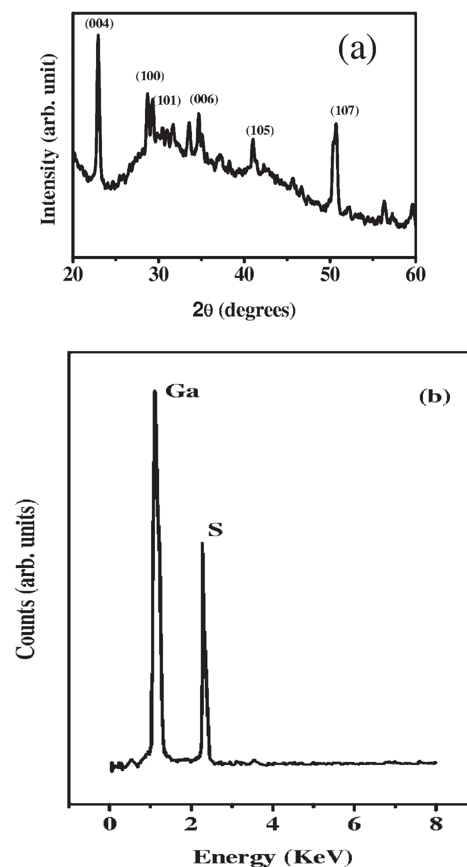

Figure 1. (a) Typical XRD pattern of as-prepared GaS nanostructures (at 700 °C). (b) EDAX spectrum of the same sample.

atmosphere, the yellow layer of GaS was observed to be deposited on the Si substrates.

The GaS samples were characterized by X-ray diffractometer (Seifert 3000P) using CuKα radiation (λ =1.54178 Å). The morphologies of the products were characterized by a scanning electron microscope (SEM, HITACHI S-2300) operated at 25 kV. The microstructure and crystal growth of the products was studied by a high-resolution transmission electron microscope (HRTEM; JEOL 2010) operated at 200 kV equipped with Energy dispersive X-ray spectrometry (EDS). The room temperature photoluminescence measurements were carried out using a spectrofluorometer (Hitachi-2500). The field emission current density-applied field (J-E) and current−time ($I-t$) measurements were carried in a custom-built metal field emission microscope. The field emission studies were carried out in a "close proximity" (also termed as "planar diode") configuration, wherein the aligned GaS nanostructure grown on Si substrate placed at 700 °C served as a cathode and a semitransparent cathodoluminescent phosphor screen as an anode. The cathode, pasted onto a copper rod using vacuum compatible conducting silver paste, was held in front of the anode screen at a distance of ~1 mm. The working chamber was evacuated using ultra high vacuum system comprising turbo molecular pump, a sputter ion pump and a titanium sublimation pump. The cathode (aligned GaS nanohorns) did not show any appreciable degassing and vacuum could be obtained with usual speed. After baking the system at 150 °C for 8 h, pressure of $\sim 1 \times 10^{-8}$ mbar was obtained. The current density−applied field (J−E) and the current−time (I-t) measurements were carried out at this base pressure using a Keithley 6514 system electrometer and a Spellman high voltage DC power supply. Special care was taken to avoid any leakage current by using shielded cables with proper grounding.

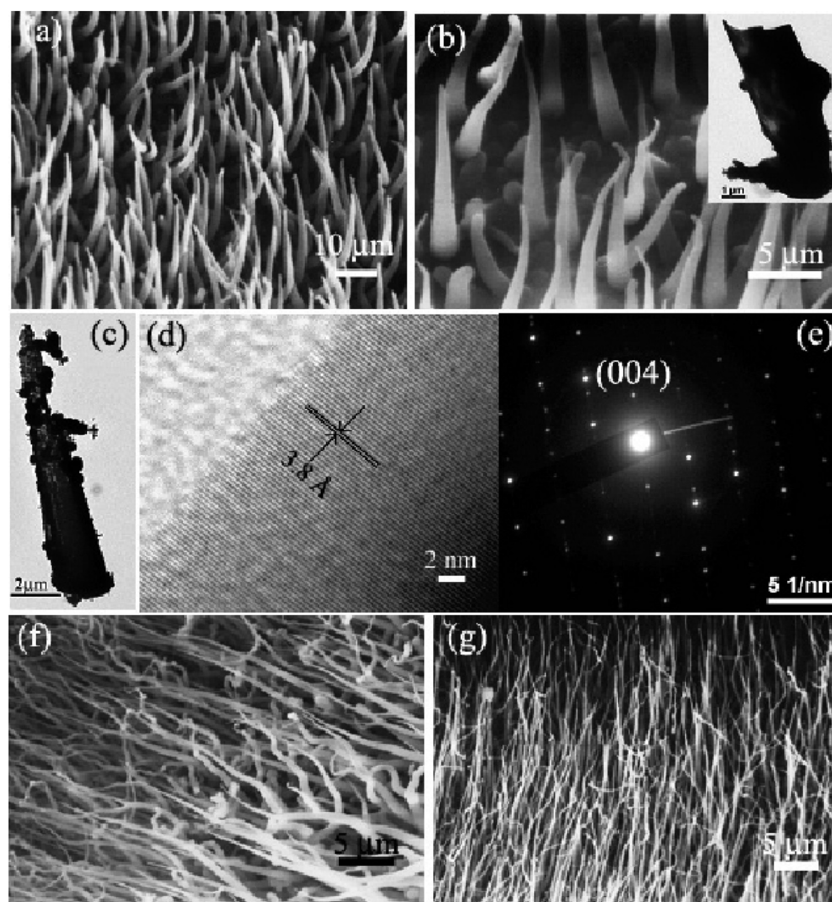

Figure 2. (a) Low- and (b) high-magnification SEM images of GaS nanohorn arrays deposited at 700 °C. Inset shows TEM of bended nanohorn. (c) TEM images of individual straight nanohorn. (d) HRTEM image from the wider part of nanohorn showing the layered structure. (e) SAED pattern of the nanohorn (HRTEM shown in d). (f) Low-magnification SEM image of elongated nanohorns formed with carrier gas flow rate 200 sccm. (g) Low-magnification SEM image of GaS nanowires formed at 700 °C with deposition time of 1 h.

3. RESULTS AND DISCUSSION

Figure 1a shows the typical XRD pattern of the as-synthesized nanohorn films, indicating the formation of hexagonal GaS phase (JCPDS card, No. 30−0576): a = 3.587 Å and c = 15.49 Å; space group: *P*63/*mmc*. The diffraction pattern indicates random orientation of nanohorn sample. The composition of the GaS nanostructures was determined by an EDAX (Figure 1b) and analysis suggests the presence of stoichiometric ratio of Ga and S elements. Figure 2a shows the SEM image of the vertically aligned GaS nanohorn arrays deposited on the Si substrate placed at the temperature around 700 °C. The basal and tip diameters of these nanohorns are nearly 2 μm and 200 nm, respectively and they are nearly 25 μm in length. Higher magnification SEM images reveal that the surface of these nanohorns is textured with GaS nanoparticles. It is seen from figure 2b that few nanohorns have a tendency to bend. Inset of Figure 2b shows a low magnification TEM image of bent nanohorn with 88° angle between both sides. It is reported previously[13] that the GaS nanoblets have a tendency to bend the growth direction at nearly 95−105° angle to the initial growth axis due to the perturbation effect of catalyst droplet diameter and minimization of surface-interfacial energy. TEM image (Figure 2c) of a straight nanohorn confirms the presence of nanoparticles on the surface. Figure 2d is the lattice-resolved HRTEM image of fringe patterns of a nanohorn having *d*-spacing of 3.8 Å, corresponding to the (004) lattice plane of GaS in hexagonal phase. The layered structure of GaS is made up of repeated S−Ga−Ga−S at 7.5 Å apart.[8,23] Two strips are seen per each S−Ga−Ga−S layer. The Ga−Ga distance within one layer is shorter than the Ga−Ga distance between two molecular sheets, so the average Ga−Ga layer is half of 7.5 Å. The fringe pattern with the *d*-spacing of 3.8 Å corresponds to the average Ga−Ga distance. Figure 2e shows the SAED pattern for the nanohorns, which suggests the single crystal nature of the nanohorns. In order to understand the effect of gas flow rate of the growth mechanism of the nanohorns, a contrastive experiment is carried out where the gas flow rate is increased to 200 sccm. The SEM image of the obtained product is provided in figure 2f. It is observed that the length and aspect ratio of nanohorns increases with increasing the flow rate. Similar results are observed with increasing the deposition time of 1 h (Figure 2g). The overall yield is decreased at the carrier gas flow rate for 50 sccm. SEM image (see Figure S1 in the Supporting Information) shows the nanohorns are not vertically upward in this condition. The SEM and TEM images of the product deposited on the Si substrate just above the Ga source at 800 °C are given in Figure 3. SEM images the product in different magnifications, show nanowires with length of several tens of micrometers length with diameter

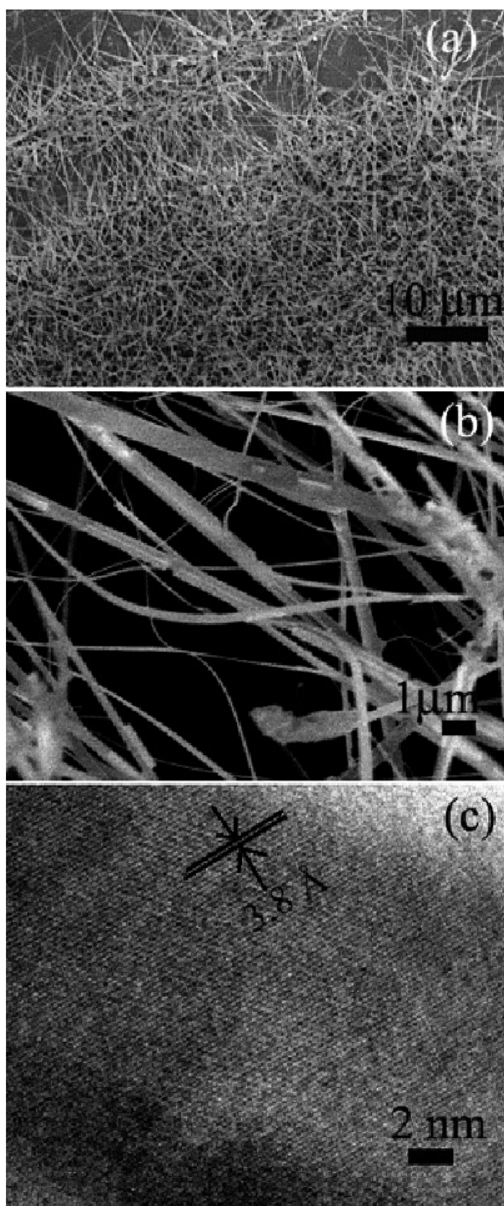

Figure 3. (a, b) SEM images of different morphologies of GaS nanowires deposited at 800 °C. (c) HRTEM images of GaS nanowires.

~300 nm. TEM study provides interesting structural information on the nanowires. HRTEM image of a typical GaS nanowire shows ripples, which may be due to lattice strain during the formation. These nanowires are single crystal in nature with the calculated interplanar spacing d is 3.8 Å, which corresponds to [004] lattice plane of hexagonal GaS.

The formation of GaS nanowires may be explained from the viewpoint of VLS process. In the first step, the Au film thermally transferred to energetically favored nanodroplets. The low vapor pressure (on the order of 1×10^{-5} atm at 900 °C)[24,25] and low ionic mobility of Ga,[26] ensure slow and steady supply of source metal molecules. The flow rate of the Ar in the present experiments is sufficient for the incoming Ga and S vapor to be absorbed in these liquid Au droplets and also reach to the substrate placed at the last end where the temperature is ~550 °C. After gradual absorption of Ga and S vapor, the liquid droplets reach a saturation concentration resulting in the growth of the nanowires in the high-temperature stable GaS phase while reducing the free energy of liquid−solid system via the Au-catalytic VLS mechanism. The VLS mechanism emphasizes that the incorporation of reactant species are at high energy sites and then diffusion to the surface ensures the growth of the nanostructures. The process may embody the intrinsic crystallography of materials into nanostructures to form well-faceted structures.[27,28] GaS being a layered structure, at the time of growth it is expected to have many dangling bonds at the edges, which can easily incorporate atoms directly carried by the gas phase or diffusion through the top/bottom surfaces. The horn shaped 1D nanostructures are generally produced under the influence of one or all of the following conditions. The formation of nanohorn structures may happen due to the gradual decrease in the supply of source materials in carrier gas. This may results in instability at relatively high growth temperature to resist decay and the droplet becomes gradually smaller as the structure grows. In another case, growth condition at high temperature and low pressure the catalytic droplet may not hold the adsorbed species on its surface resulting in the diffusion of adsorbed species via the sidewall of the nanostructure.[29−31] The rough surface of GaS nanohorns indicates the occurrence of vapor-solid (VS) process along with VLS. The quenching from high temperature to room temperature may results in simultaneous nucleation and less formation of low energy smooth surface.[32]

The substrate temperature as well as their position with respect to source metal, plays important roles in the formation of GaS nanostructures with different morphologies. In order to study the effect of the substrate position, we studied the GaS product deposited on Si substrate position at 550 °C. Figure S2a in the Supporting Information shows the SEM image of GaS products deposited at this position consists of microspheres with diameter of nearly 200 nm and inset shows the high-magnification image of a microsphere with very smooth surface. Panels b and c in Figure S2 in the Supporting Information show TEM images of the microspheres with different magnifications. Although we could not find any trace of broken spheres, the contrast between dark and pale inner part in Figure S2c in the Supporting Information provides a proof for hollow nature of these spheres. The size and wall thickness of these spheres, measured from aforementioned image, are nearly 230 and 50 nm, respectively. The SAED pattern (inset in Figure S2c in the Supporting Information) of these spheres shows ringlike pattern indicating that these GaS spheres are polycrystalline in nature. The concentric rings can be assigned to (107) planes of hexagonal GaS crystal structure.

Photoluminescence (PL) spectrum of GaS nanohorns at room temperature, recorded at excitation wavelength of 350 nm is shown in Figure 4. The luminescence of GaS nanohorns showed a nonsymmetric and broad PL spectrum with a maximum emission peak position at 452 nm and another shoulder at ~495 nm. GaS has a direct band gap at 3.05 and an indirect band gap at 2.59 eV, so the peaks at 452 and 495 nm are localized in the energy range of direct and indirect gaps, respectively. The origin of the PL may be attributed mainly to structural defects such as S vacancy, Ga vacancy and stacking defects.[33] During the photoexcitation process, the electron in a donor, which mainly originates from S vacancy, can be captured by the excited hole on an acceptor formed by Ga vacancy, thus a photon is emitted via the radiative recombination of donor−acceptor pair.[33,34] The

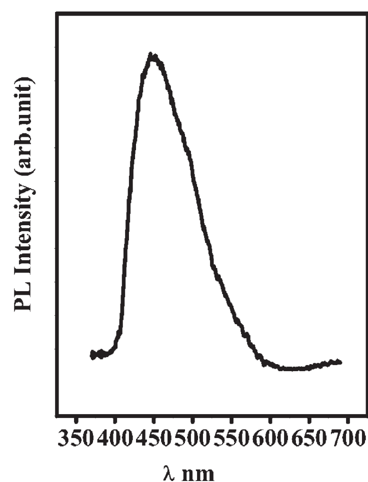

Figure 4. PL spectrum of GaS nanohorn arrays.

stacking faults present in the nanohorns may provide additional recombination sites for the observed luminescence.

Field emission is known to be sensitive to the alignment and morphology of the emitter.[1] The studies of field emission properties of different of CdS nanotips,[5] nanoneedles of AlN[35] and ZnO[20] show that the lower turn on voltage depends on the aspect ratio and alignment. It is reported that the FE behavior of GaS nanobelts showed a very small turn-on field of ~2.9 V/μm (1 nA/cm^2) which is attributed to their sharp edges and high aspect ratio.[13] The GaS nanohorn arrays with relatively sharp tips are expected to be good field emitter. The field emission current density-applied field (J−E) characteristic of the GaS nanohorn arrays is depicted in Figure 5a. The turn-on field, defined as the field required drawing an emission current of ~0.1 μA/cm^2, is found to be ~4.2 V/μm. The emission current increases rapidly with increasing the applied voltage. An emission current density of ~19 μA/cm^2 has been drawn at an applied field of ~7.4 V/μm. Analysis suggests that the exploration of the GaS nanostructures as field emitters is rather limited, however, the turn-on field value in present study for the GaS nanohorns array is found to be comparable to the other sulfides such as aligned CdS nanowires (7.8 V/μm, for 0.1 μA/cm^2)[35] and multipods (7.2 V/μm, for 0.1 μA/cm^2),[36] ZnS nanobelts (3.8 V/μm, for 10 μA/cm^2),[37] and ZnO nanowires (5 V/μm, for 10 μA/cm^2),[38] nanonails, nanopencils (7.9,7.2 V/μm, for 10 μA/cm^2)[39] field emitters. Therefore, the vertical alignment, the sharp tips of these GaS nanohorns attribute the better filed emission behavior in terms of lower turn-on than GaS nanobelts.[13] In the present case, the current density (J) is estimated by considering the entire area of the emitter (1 cm^2). The F−N plot, i.e., ln (J/E^2) versus ($1/E$), derived from the observed J−E characteristic is shown in Figure 5b. The F−N plot shows overall linear behavior with decrease in the slope (saturation tendency) with applied field range. Such type of F−N plot shows tendency toward saturation at very high applied field which is consistent with previous results.[13,35] For field emission electron sources, along with the emission competence, the current stability is also a decisive and an important parameter. I−t plot recorded at the base pressure of 1×10^{-8} mbar is shown in Figure 5c. The emission current stability of the GaS nanohorn array emitter has been investigated at the preset current value of ~1 μA (at applied voltage of ~5.2 kV) over the duration of more than 4 h. It can be seen that the emission current initially increases as shown in the inset (A) of figure 5c and then stabilizes to a higher value of ~2.5 μA. This can be attributed to the preconditioning of the emitter, as the field emission is a surface sensitive phenomenon and it requires preconditioning by removal of the adsorbed species. After stabilization, the current fluctuations are seen to be smaller. The fluctuations are in the form of 'spikes', such as digital pulse, which may be attributed to the adsorption and diffusion of residual gas molecules on the emitter surface. The emitter surface would become cleaner because of the ion bombardment induced desorption of the residual gases, and the clean surface thus produced leads to stabilization of the emission current at a higher value.[13,40] The striking feature of the field emission behavior of the GaS nanohorn arrays is that the average emission current remains nearly constant over the entire duration without degradation. This is an important feature, particularly from the practical application of the emitter material as an electron source. Inset A of Figure 5c shows that the emission current is very stable with the time. A typical field emission image, captured at the applied field of ~6 V/μm is shown as in the inset B of Figure 5c. The image shows a number of tiny spots, which correspond to emission from the most protruding GaS nanohorn arrays. The temporal changes in the intensity of the spots are observed to be commensurate with the emission current fluctuation as seen in the I−t plot. GaS nanohorns are grown on the Si substrate which could be integrated to the Si based technology.

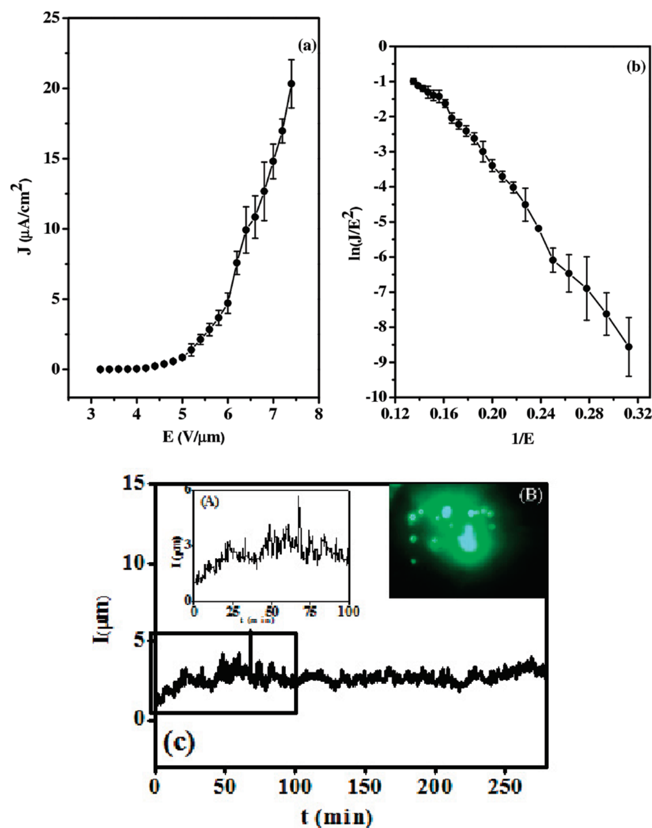

Figure 5. (a) Field emission current density−applied field (J−E) plot of the GaS nanohorns (b) corresponding Fowler−Nordheim (F−N) plot. (c) Field emission current stability (I−t) plot of GaS nanohorns (inset A shows the initial fluctuation in the emission current and inset B shows a typical field emission image).

4. CONCLUSIONS

In summary, GaS nanostructures with different morphologies are fabricated through a VLS mediated thermal evaporation method. The morphology of GaS nano and microstructures are varied from nanowires, nanohorn arrays to microspheres by varying the temperature. The turn-on field value of GaS nanohorns array is found to be the low turn-on field 4.2 V/m having current density of 0.1 μA/cm^2. The F−N plot shows a nonlinear nature in the entire range of the applied field. The emission current stability measurements indicate the stability for more than 4 h. We anticipate that the present GaS nanohorn arrays are promising candidates for future application in field-emission-based devices.

■ ASSOCIATED CONTENT

Supporting Information. S1 shows the SEM image of scattered GaS nanohorns at 700 °C with carrier gas flow rate of 50 sccm. S2 shows the SEM (a) and TEM images (b and c) of GaS microspheres prepared at 550 °C. This material is available free of charge via the Internet at http://pubs.acs.org.

■ AUTHOR INFORMATION

Corresponding Author

*E-mail: msap@iacs.res.in. Phone: (91)-33-2473-4971. Fax: (91)-33-2473-2805.

■ ACKNOWLEDGMENT

The authors pay their tribute to Late Prof. Subhadra Chaudhuri, who was a constant inspiration behind this work. Anuja Datta is thankful to CSIR, Government of India, for providing the financial support. P.G.C. is thankful to the UGC, India, for the award of Rajiv Gandhi National Fellowship. D.S.J. thanks C.SIR for Emeritus Scientist scheme.

■ REFERENCES

(1) Zhai, T.; Fang, X.; Bando, Y.; Liao, Q.; Xu, X.; Zeng, H.; Ma, Y.; Yao, J.; Golberg, D. *ACS Nano* **2009**, *3*, 949–959.

(2) Fernelius, N. C. *Prog. Cryst. Growth Charact.* **1994**, *28*, 275–353.

(3) Coehoorn, R.; Haas, C.; Dijkstra, J.; Flipse, C. J. F.; deGroot, R. A.; Wold, A. *Phys. Rev. B* **1987**, *35*, 6195–6202.

(4) Xiaosheng, F.; Bando, Y.; Meiyong, L.; Zhai, T.; Gautam, U.; Li, L.; Koide, Y.; Golberg, D. *Adv. Funct. Mater.* **2010**, *20*, 500–508.

(5) Zhai, T.; Fang, X.; Bando, Y.; Dierre, B.; Liu, B.; Zeng, H.; Xu, X.; Huang, Y.; Yuan, X.; Sekiguchi, T.; Golberg, D. *Adv. Funct. Mater.* **2009**, *19*, 2423–2430.

(6) Gasanly, N. M.; Aydinli, A.; Ozkan, H.; Kocabas, C. *Solid State Commun.* **2000**, *116*, 147–151.

(7) Köhler, Th.; Frauenheim, Th.; Hajnal, Z.; Seifert, G. *Phys. Rev. B* **2004**, *69*, 193403–4.

(8) Lieth, R. M. A. *Preparation and Crystal Growth of Materials with Layered Structures*; D. Reidel: Dordrecht, The Netherlands, 1977.

(9) Gautam, U. K.; Vivekchand, S. R. C.; Govindaraj, A.; Kulkarni, G. U.; Selvi, N. R.; Rao, C. N. R. *J. Am. Chem. Soc.* **2005**, *127*, 3658–3659.

(10) Hu, J. Q.; Bando, Y.; Zhan, J. H.; Liu, Z. W.; Golberg, D. *Appl. Phys. Lett.* **2005**, *87*, 153112–3.

(11) Gautam, U. K.; Vivekchand, S. R. C.; Govindaraj, A.; Rao, C. N. R. *Chem. Commun.* **2005**, 3995–3997.

(12) Hu, P. A.; Liu, Y. Q.; Fu, L.; Cao, L. C.; Zhu, D. B. *Appl. Phys. A: Mater. Sci. Process.* **2005**, *80*, 1413–1417.

(13) Panda, S. K.; Datta, A.; Sinha, G.; Chaudhuri, S.; Chavan, P. G.; Patil, S. S.; More, M. A.; Joag, D. S. *J. Phys. Chem. C* **2008**, *112*, 6240–6244.

(14) Shen, G.; Chen, D.; Chen, P. C.; Zho, C. *ACS Nano* **2009**, *3*, 1115–1120.

(15) Lin, C.; Yu, G.; Wang, X.; Cao, M.; Lu, H.; Gong, H.; Qi, M.; Li, A. *J. Phys Chem C* **2008**, *112*, 18821–18824.

(16) Gautam, U. K.; Fang, X.; Bando, Y.; Zhan, J.; Golberg, D. *ACS Nano* **2008**, *2*, 1015–1021.

(17) Liu, N.; Wu, Q.; He, C.; Tao, H.; Wang, X.; Lei, W.; Hu, Z. *ACS Appl. Mater. Interfaces* **2009**, *1*, 1927–1930.

(18) Zhai, T.; Li, L.; Ma, Y.; Liao, M.; Wang, X.; Fang, X.; Yao, J.; Bando, Y.; Golberg, D. *Chem. Soc. Rev.* **2011**, *40*, 2986–3004.

(19) Zhai, T.; Ye, M.; Li, L.; Fang, X.; Liao, M.; Li, Y.; Koide, Y.; Bando, Y.; Golberg, D. *Adv. Mater.* **2010**, *22*, 4530–4533.

(20) Zhao, Q.; Zhang, H. Z.; Zhu, Y. W.; Fang, S. Q.; Sun, X. C.; Xu, J.; Yu, D. P. *Appl. Phys. Lett.* **2005**, *86*, 203115–3.

(21) Shen, G. Z.; Bando, Y.; Liu, B. D.; Golberg, D.; Lee, C. J. *Adv. Funct. Mater.* **2006**, *16*, 410–416.

(22) Ye, C. H.; Bando, Y.; Fang, X. S.; Shen, G. Z.; Golberg, D. *J. Phys. Chem. C* **2007**, *111*, 12673–12676.

(23) Ho, C. H.; Lin, S. L. *J. Appl. Phys.* **2006**, *100*, 083508–6.

(24) Lide, D. R. *Handbook of Chemistry and Physics*; CRC Press: Boca Raton, FL, 1996.

(25) Geiger, F.; Busse, C. A.; Loehrke, R. I. *Int. J. Thermophys.* **1987**, *8*, 425–436.

(26) Phillips, J. C. *Phys. Rev. B* **1993**, *47*, 2944–2949.

(27) Ye, C. H.; Fang, X.; Hao, Y. F.; Teng, X. M.; Zhang, L. D. *J. Phys. Chem. B* **2005**, *109*, 19758–19765.

(28) Hao, Y.; Meng, G.; Wang, Z. L.; Ye, C.; Zhang, L. *Nano Lett.* **2006**, *6*, 1650–1655.

(29) Mohammad, S. N. *J. Chem. Phys.* **2006**, *125*, 094705–16.

(30) He, M.; Mohammad, S. N. *J. Chem. Phys.* **2006**, *124*, 064714–7.

(31) He, M.; Mohammad, S. N. *J. Vac. Sci. Technol., B* **2007**, *25*, 940–5.

(32) Mohammad, S. N. *Nano Lett.* **2008**, *8*, 1532–1538.

(33) Shigetomi, S.; Ikari, T. *J. Appl. Phys.* **2007**, *102*, 033701–033704.

(34) Belenkii, G. L.; Godzhaev, M. O. *Phys. Status Solidi B* **1978**, *85*, 453–458.

(35) Song, X.; Guo, Z.; Zheng, J.; Li, X.; Pu, Y. *Nanotechnology* **2008**, *19*, 115609–6.

(36) Zhang, M.; Zhai, T.; Wang, X.; Ma, Y.; Yao, J. *Cryst. Growth Des.* **2010**, *10*, 3–6.

(37) Lu, F.; Cai, W. P.; Zhang, Y. G.; Li, Y.; Sun, F. Q.; Heo, S. H.; Cho, S. O. *Appl. Phys. Lett.* **2006**, *89*, 231928–3.

(38) Lin, C. C.; Lin, W. H.; Li, Y. Y. *J. Phys. D: Appl. Phys.* **2008**, *41*, 225411–6.

(39) Chen, S. J.; Liu, Y. C.; Shao, C. L.; Mu, R.; Lu, Y. M.; Zhang, J. Y.; Shen, D. Z.; Fan, X. W. *Adv. Mater.* **2005**, *17*, 586–590.

(40) Sinha, G.; Datta, A.; Panda, S. K.; Chavan, P. G.; More, M. A.; Joag, D. S.; Patra, A. *J. Phys. D: Appl. Phys.* **2009**, *42*, 185409–6.